

Nearshore density-driven exchange flow between open water and vegetation: A Laboratory study

Y.T. Lin¹

¹ Ocean College, Zhejiang University, 316021, Zhoushan, China

Abstract

Laboratory lock exchange experiments are presented to study the density-driven exchange flow between open water and adjacent vegetation over a sloping bottom. Rigid and emergent cylinders are used to represent the canopy region such as reeds in aquatic environments. A model canopy occupying only in one side of the channel can result in variations of speeds of current head and tail, subsequently creating different flow patterns. For a model canopy in shallows and open water in deep regions, dense fluid trapped in shallows can lead to less dense fluid flow into the current head, causing the current head to possibly separate from the current body and greater downslope speed of the current head. For a model canopy in deeper regions but open water in shallows, dense fluid can possibly be jammed in front of the model canopy, which increases the thickness of dense fluid at the center of the channel. Since the dense fluid can be regarded as a deformable and continuous fluid body, the current motion in one side can somehow be influenced by that in the other side.

Introduction

In aquatic environments, convective exchange flows play an important role to transport nutrient, pollutants and chemical substances between the littoral and pelagic regions of lakes or reservoirs in the absence of wind or other momentum sources (e.g. river flows) [1]. The convective exchange flows are mainly driven by a density difference in the horizontal direction, which can be caused by topographic changes in nearshore [2], vegetation shading [3], or turbid patches in water [4]. The circulation induced by topographic effects is mostly common in typical field conditions. During the day the spatially uniform solar radiation leads to warmer water in shallows than that in the adjacent deeper regions, so temperature contrast between the shallow and deep waters thus develops to produce subsequent variations of water density, generating convective water exchange [5]. During nighttime, the condition is reversed that shallow regions cool relatively more quickly than deeper regions, leading to cooler water temperature in shallows rather than that in deep regions, which can drive opposite convective circulation to that during the day [5].

Shading from emergent or floating vegetation can also affect water temperature that subsequently results in differential heating and cooling between vegetated regions and open water [6]. Dense vegetative stands can intercept more incident sunlight which causes cooler water temperature in vegetated areas rather than in adjacent open water during daytime [7]. Similarly, during nighttime, emergent vegetation can reduce radiation losses so that water in the open region is cooler than that in the vegetated region [8]. Previous literatures indicated that the temperature differences between the vegetated regions and open water can be sufficiently large (max. $\Delta T \approx 2\sim 4^\circ\text{C}$) to produce evident temperature gradients and establish a near-surface flow from the illuminated to the shaded regions. [7,8]. Löfstedt and Bengtsson [7] observed that the exchange surface flow between emergent vegetation (reeds) and open water can be up to 1.5 cm/s in littoral zones of a

lake. Tanino et al. [3], Zhang and Nepf [3] and Zhang and Nepf [9] modelled the vegetative drag using a most commonly quadratic law over a flatbed. However, littoral aquatic vegetation is commonly observed over a sloping bottom, instead of a flat bottom, and vegetation distribution is non-uniform from onshore to offshore because of variations of light and nutrient supplies at different water depths [10]. To the best of authors' knowledge, only fewer studies investigated the combined effects of topography and vegetation shading on density-driven flows.

Recently, Ho and Lin [11] conducted lock-exchange experiments over a slope within uniformly emergent and rigid vegetation. Assuming the distribution of hydrostatic pressure within gravity currents, a formula including the slope and vegetation drag to estimate the speed of current head is developed. They also revealed that the head would accelerate over the downslope course if the cylinder density is less than 2%. However, dynamic features of density current within non-uniformly distributed vegetation, i.e., vegetation in one side and open water, are not examined. Also, exchange flowrates, the quantities of greatest interest on transport of nutrients, pollutants, and chemical substances, were drawn less attention in their study.

This study is an extension of Ho and Lin [11]'s work that only focuses on convective exchange flow within unfirmly distributed canopy. Lock exchange experiments are conducted in which the density difference between the two sides of an inclined channel is constant. Various experimental configurations such as vegetation in both sides and vegetation in either side of the channel are included to represent different field conditions. In comparison to Ho and Lin [11]'s work, the new configuration (a model canopy in one side and open water in the other side) can better simulate the field conditions, where exchange flow is more likely to be produced by differential shading. As Zhang and Nepf [9] stated, although the experiment is a simplification of the field situation in which the density difference varies over the course of the diurnal heating, the setup and transient time scale for the exchange flow is short compared to the time scale of diurnal temperature variations. This results from the simplified experiments are thus still reasonable and feasible to evaluate the scales of current speeds and exchange flowrates.

Experimental Methods

The wedge-shaped channels used in the experiments were made with a rectangular cross-section 0.25 m wide, 0.8 m long and different bottom slopes with transparent Plexiglas sidewalls. Three different slopes S_0 of 0.075 (~4.3 degrees), 0.125 (~7.1 degrees), and 0.25 (~14.0 degrees), corresponding to the maximum heights H of 6 cm, 10 cm, and 20 cm are chosen. All channels were separated into two regions of equal length by a removable and 5 mm thick partition. Rigid wood sticks (diameter d of 0.3 cm) and chopsticks (diameter d of 0.5 cm) were used to model rigid and emergent aquatic vegetation which typically has a diameter $d=0.1$ to 1 cm. PVC (Polyvinylchloride) sheets perforated with uniformly distributed holes were placed on top of the channel to locate the model vegetation. The wood sticks or chopsticks were pushed

through the holes and extended down to the channel bottom. There is a 0.5-cm gap between the perforated sheet and water surface to prevent the friction from the upper PVC sheets. In this study, different experimental configurations including a model canopy either in shallow or deeper regions and the other side of open water are considered (see Fig.1). To compare the cases of a model canopy only in one side of the channel, some cases were carried out when the model canopies occupy in both sides of the channel or there is no model canopy in the channel.

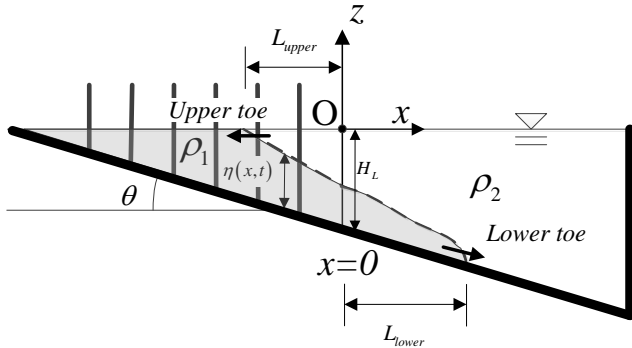


Figure 1 Schematic of a lock-exchange experiment within a cylinder array in shallow regions.

The density of model canopy ϕ ranges between 0 and 0.069, producing the dimensionless array density $ad = 0$ to 0.088, which is comparable to the ad values for natural canopies between 0.01 to 0.1 [12]. The shallow region was filled with well-mixed saltwater of density ρ_1 , and the deep regions was filled with freshwater of density ρ_2 . For flow visualization, saltwater was dyed with dark-color food dye. The images of flow patterns were captured by a Canon VIXIA HF R400 camcorder (1920 × 1080 pixel resolution at 30 fps). The foremost part of currents, in the lower and upper layers were identified using a commercial software Matlab. The details of the experimental procedures and subsequent analysis of the recorded images can be referred to Ho and Lin [11]. Because the dense fluid is filled in shallow regions, experiments performed are to represent field conditions that water temperature is cooler in shallows than that in deep regions. Hence, a model canopy in shallow or deep regions are able to simulate convective water exchange in two conditions: (1) for a model canopy in shallows, experiments incline to mimic exchange flow during daytime, and (2) experiments of a model canopy in deeper regions but dense fluid in shallows allows to model exchange flow during nighttime. The heat fluxes of daytime heating and nighttime cooling are usually considered equal, so experimental results can be applied to the entire diurnal cycles whether vegetation is in shallow or deep sides.

Results

Gravity current started to propagate after the lock gate was removed. Fig. 2 presents the temporal evolution of the interface on a 4.3° slope at the same reduced gravity ($g' = 2.1 \text{ cm/s}^2$), but the model canopy ($\phi=6.9\%$) only occupied in shallow or deep regions and the other side is open water. When the model canopy in deep regions and open water in shallows, gravity current moving into the shallows is against the slope and thus decelerates with time. The interface profiles of the current in shallows perform more like a parabolic shape rather than a semi-elliptic shape (Fig.2a). Since the model canopy is in deep regions, canopy-induced drag reduces the downslope current speed, allowing less fluid into the model canopy. Gravity current thus accumulates right before the model canopy, leading the increases of the thickness of the gravity current at $x = 0$ (Fig.2a). The interface profiles within the model canopy

gradually perform linear patterns as the current moves more into the model canopy. The classic semi-elliptical shape of the current head can only be found in the very front as reported by Ho and Lin [23]. On the other hand, for the case of open water in deep regions and the model canopy in shallows, the interface profiles in shallows perform like an inclined straight line. In deep regions, the classic semi-elliptical shape of the gravity current head is evidently performed when the current descends down an unvegetated slope (Fig.2b). The gravity and buoyancy work in concert to accelerate the current. As the flow descends down the slope, mixing and entrainment of the currents with the ambient fluids progressively occurs (Fig.2b). In the meantime, the thickness of the gravity current at $x = 0$ maintains nearly constant.

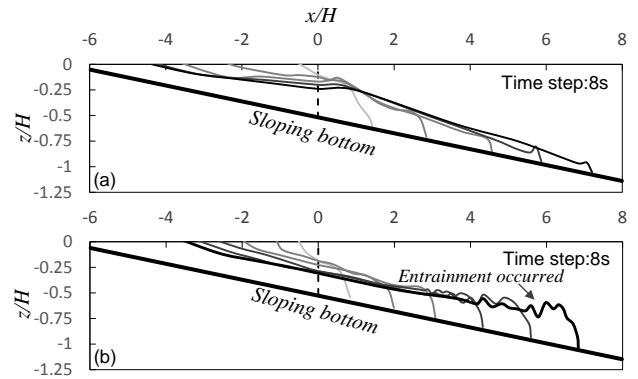


Figure 2 Temporal progression of the interface at a slope of 0.075 (~4.3°) and $g'=2.1 \text{ cm/s}^2$. (a) $\phi = 0\%$ in shallows and $\phi = 6.9\%$ in deep regions, and (b) $\phi = 6.9\%$ in shallows and $\phi = 0\%$ in deep regions. The dash line is the location of the lock and the time interval between each profile is provided on the top of each figure.

The temporal evolutions of the upper and lower toe locations of gravity current are shown in Fig.3, where $\bar{H} (= \frac{1}{2} H)$ is the mean water depth, i.e., the depth at the lock ($x = 0$). After the gate removal, the current will experience an unsteady period (also called the initial effect [13]) until the semi-elliptical head is formed. The toe locations during this period are indistinct to be identified, so the data during the initial period are excluded in Figs.3 and 4. Four configurations including no model canopy, model canopies in both sides, and a model canopy in shallow or deep sides are compared. As expected, current of lower toe moves fastest when there is no model canopy in both sides (black line in Fig.3a), whereas the current within model canopies in both sides propagates slowest among the four scenarios (grey line in Fig.3a). Generally, the lower toe current can travel further distance that the lower toe current does because buoyancy and gravity work together in the lower toe current. The downslope current speeds when a model canopy in deep regions (black-dash line in Fig.3a) is faster than that when a model canopy in shallows (grey-dash line in Fig.3a). The possible explanation is that when a model canopy occupies in deep regions, the areas that water can pass through are reduced, which increases the current speeds. For the upper toe, the density current accelerates at the beginning and then gradually decelerates for all four configurations (Fig.3b). This can be attributed to viscosity that takes effect as the current move more into the tip of the domain. i.e., smaller water depth. Viscosity gradually becomes the dominant mechanism to determine the current velocity in shallows as Lin and Wu [14] revealed. When there are no model canopy in both sides, current speed of upper toe is faster than the other three cases at the beginning stage and gradually declines due to viscosity. For a model canopy in deep regions but open water in shallows, the speed of the upper toe at a later stage can surpass that without model canopies in both sides. The speed of upper toe current is slowest among four configurations when a model canopy is only present in shallows.

This is possibly affected by the lower toe current which moves fast into the deep region and brings the whole current body (dense fluid) to the deep regions. Since the dense fluid can be regarded as a deformable and continuous body, the current motion in one side can possibly be influenced by that in the other side. Without model canopies in both sides, the centroid of the deformable body still moves down the slope. However, when vegetation only occupies in one side and the other side is kept open, the movement of the centroid of the dense body becomes complicated, possibly altering the motions of the upper and lower toes of the current.

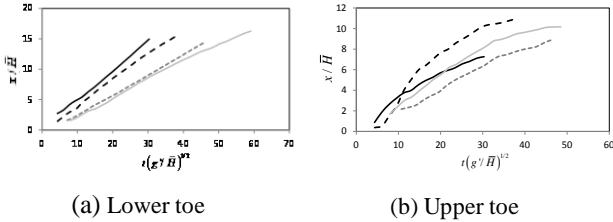


Figure 3 Temporal evolution of the lower and upper toe positions at a slope of 0.075 ($\sim 4.3^\circ$) and $g'=2.1 \text{ cm/s}^2$. Note: “—”: no model canopy, “- -”: 6.9% model canopy in both sides, “- · -”: 6.9% model canopy in deep regions, and “· · ·”: 6.9% model canopy in shallows.

Fig. 4 displays the temporal evolutions of the upper and lower toe locations of gravity current at a larger reduced gravity ($g' = 7.1 \text{ cm/s}^2$). In the lower toe, the slopes of $x-t$ curve for the four configurations are approximately the same, meaning that the downslope current velocities are similar irrespective of distribution of model canopies. Regarding the case of vegetation only in deep regions, a notable deceleration of lower toe occurs at a dimensionless time from 12 to 17. For the upper toe in Fig.4b, the $x-t$ curves for four configurations also exhibit similar slopes, indicating the similar current speed in the upper toe. In addition, the $x-t$ curves show fluctuating patterns, which implies the temporal variations of current speeds. The results also show that the upper toe current when a model canopy is present in deep regions can move as far as that without a model canopy, whereas the upper toe currents of a model canopy occupies in shallows or in both regions can propagate the similar distance until the low toe current of a model canopy in shallows reaches the end of the flume.

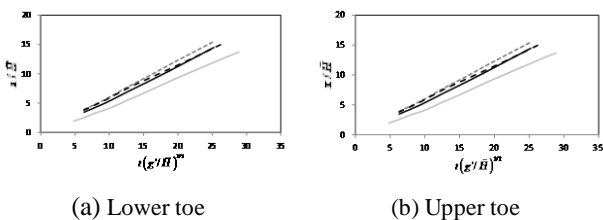


Figure 4 Temporal evolution of the lower and upper toe positions at a slope of 0.075 ($\sim 4.3^\circ$) and $g'=7.2 \text{ cm/s}^2$. Note: “—”: no model canopy, “- -”: 6.9% model canopy in both sides, “- · -”: 6.9% model canopy in deep regions, and “· · ·”: 6.9% model canopy in shallows.

As the reduced gravity and channel slope become larger, the interfacial profiles of gravity current exhibit different patterns (Fig.5). For a model canopy only in deep regions, dense fluid in shallows rapidly descends but is jammed in front of the model canopy, causing the rising interface at the center of the channel ($x = 0$) (Fig.5a). As the current gradually flows into the model canopy, the risen interface at the center of the channel then decreases. For the vegetation in shallows, on the contrary, the current thickness at the center of the channel rapidly reduces as the current moves into the open and deep regions (Fig.5b). The thinning current thickness shows the tendency of the current head

detaching (or separating) from the current body as Nogueira et al. [15] mentioned gravity currents over a rough flatbed. The reason responsible for separation tendency is because the dense fluid is trapped within a model canopy and cannot immediately supply enough fluid into the current head. Without enough fluid supplies, the current head moves as an individual body and accelerates along the downslope course. The tendency of separation between the lead and trailing parts of the density current can lead to greater downslope speed but less exchange volume discharge in comparison to the case of model canopy in deep regions. This phenomena can be observed more clearly from the current thickness h_d at the center of the channel (Fig.6). The dimensionless scales used on Fig.6 are: dimensionless time $\hat{t} = t \sqrt{\frac{g'}{H}}$, and dimensionless current thickness $\hat{h} = \frac{h_d}{H}$. For a model canopy in shallows and open in deep regions, \hat{h} performs an exponential decay with various speeds as \hat{t} increases (Fig.6a). This reflects the consequences of current tails trapped within the model canopy. The thinner of the current thickness confirms that the separation tendency between the current head and body. The experimental results can be manually categorized as separating and unseparating cases. Herein, “separating” means that the current head is separating from the current body with its rapidly reducing thickness at the center of the channel but not yet separate from the current body. The separation phenomena is dependent on the difference of speeds between the current head and tail, which are determined by the channel slope, reduced gravity, and canopy density in shallows. However, it is difficult to determine the separation criteria due to insufficient datasets so far.

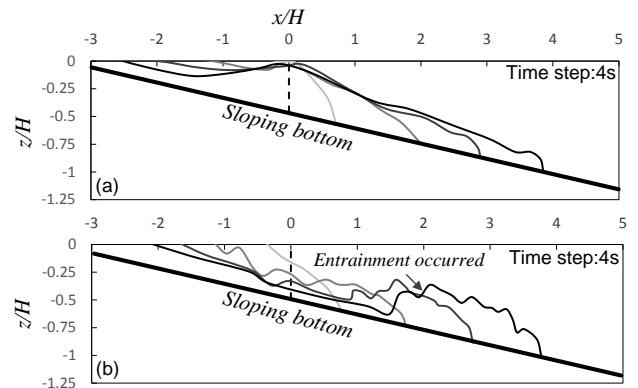


Figure 5 Temporal progression of the interface at a slope of 0.125 ($\sim 7.1^\circ$) and $g'=7.2 \text{ cm/s}^2$. (a) $\phi = 0\%$ in shallows and $\phi = 6.9\%$ in deep regions, and (b) $\phi = 6.9\%$ in shallows and $\phi = 0\%$ in deep regions.

When a model canopy is present in deep regions, \hat{h} versus \hat{t} data show two different groups: one group with higher \hat{h} values, and the other group with lower \hat{h} values, but \hat{h} values from the two groups decrease as \hat{t} increases at similar paces (Fig.6b). The data with higher \hat{h} values indicate that the dense fluid cannot swiftly flow through the model canopy, i.e., the dense fluid will be jammed in front of the model canopy. The reason for fluid jammed can be attributed to the slower current head speed but faster current tail speed. In contrast, the data with smaller \hat{h} values suggest that the density current can flow down the slope without difficult. In Fig.6b, the runs conducted on conditions without model canopy or with uniformly distributed model canopy are also compared. The results show that when a sparse model canopy ($\phi = 2.1\%$) in deep regions, \hat{h} versus \hat{t} data are similar to those conducted on conditions without a model canopy or with a uniformly distributed model canopy. In other words, the sparse vegetation in deep regions will almost pose no effects on $\hat{h} - \hat{t}$ data. However, if the reduce gravity is small and channel slope is gentle, sparse

vegetation in deep regions can also rise the $\hat{h} - \hat{t}$ data (see symbol ‘-’ on Fig.6b). It can be therefore concluded that fluid jamming occurs when only vegetation is present in deep regions, and the channel slope, reduced gravity and vegetation density in deep regions are also the key factors to result in significant differences between current head and current tail speeds as well as subsequent fluid jamming.

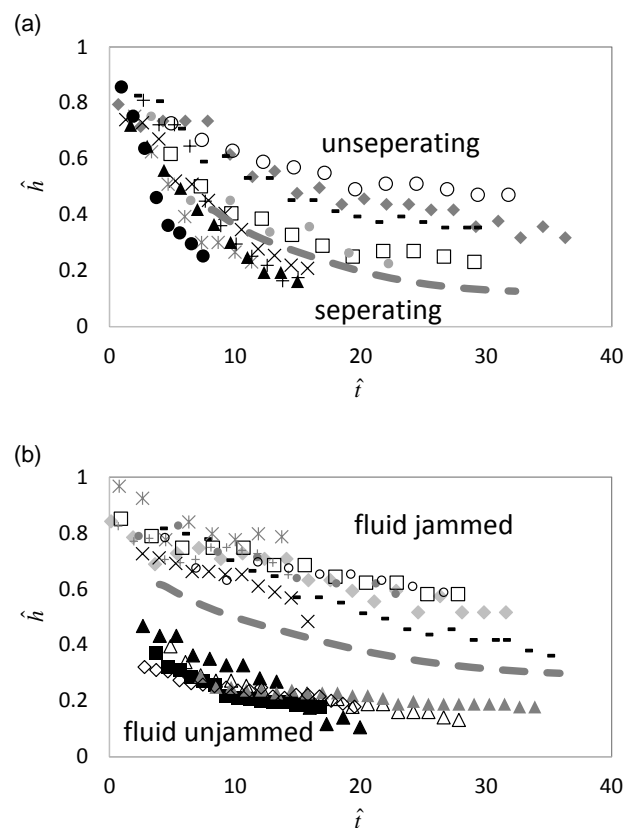


Figure 6 Normalized temporal variation of current thickness at the center of the channel (a) a model canopy in shallows, and (b) a model canopy in deep regions.

Conclusions

Lock exchange experiments are conducted to study the density-driven exchange flow between open water and adjacent vegetation over a sloping bottom. A model canopy occupying only in one side of the channel can result in variations of speeds of current head and tail, subsequently creating different flow patterns. For a model canopy in shallows and open water in deep regions, dense fluid trapped in shallows can lead to less fluid into the current head, causing the current head to possibly separate from the current body and greater downslope speed of the current head. On the other hand, for a model canopy in deeper regions but open water in shallow, dense fluid can possibly be jammed in front of the model canopy, which increases the thickness of dense fluid at the center of the channel. Since the dense fluid can be regarded as a deformable and continuous body, the current motion in one side can somehow be influenced by that in the other side.

References

[1] James WF, Barko JW. Estimation of phosphorus exchange between littoral and pelagic zones during nighttime convection circulation. *Limnol. Oceanogr.*, **36**(2),1990, 179–187.

[2] Monismith SB, Imberger J, Morison ML. Convective motion in the sidearm of a small reservoir. *Limnol. Oceanogr.*, **35**, 1990, 1676–1702.

[3] Zhang X, Nepf HM. Thermally-driven exchange flow between open water and an aquatic canopy. *J. Fluid Mech.*, **632**, 2009, 227–43.

[4] Coates M, Patterson, JC. Unsteady natural convection in a cavity with non-uniform absorption of radiation. *J. Fluid Mech.*, **256**, 1993,133–161.

[5] Farrow DE, Patterson JC. On the response of a reservoir sidearm to diurnal heating and cooling. *J. Fluid Mech.*, **246**, 1993, 143–61.

[6] Chimney M, Wenkert L, Pietro K. Patterns of vertical stratification in a subtropical constructed wetland in south Florida (USA). *Ecol. Eng.*, **27**, 2006, 322–330.

[7] Löfstedt C, Bengtsson L. Density-driven current between reed belts and open water in a shallow lake. *Water Resour. Res.*, **44**(10), 2008, W10413.

[8] Pokorný J., Kvet J. Aquatic plants and lake ecosystem, in *The Lakes Handbook*, vol. 1, edited by P. E. O’Sullivan and C. S. Reynolds, pp. 309– 340, Blackwell, Malden, Mass, 2004.

[9] Zhang X, Nepf HM. Density driven exchange flow between open water and an aquatic canopy. *Water Resour. Res.*, **44**(8), 2008, W08417.

[10] Wietzel RG. *Limnology*, Academic Press, 2001.

[11] Ho HC, Lin YT. Gravity currents over a rigid and emergent vegetated slope. *Adv. Water Resour.*, **76**, 2015, 72–80.

[12] Kadlec J. Overland flow in wetlands: vegetation resistance. *J. Hydraul. Eng.*, **116**(5), 1990, 691–706.

[13] Linden P. Theory of oceanic buoyancy-driven flow. In: Chassignet E, Cenedesse C, Verron J, editors. *Buoyancy-driven flows*. New York, NY: Cambridge University Press; 2012. 13–51.

[14] Lin YT, Wu CH. The role of rooted emergent vegetation on periodically thermal-driven flow over a sloping bottom. *Environ. Fluid Mech.*, **14**, 2014, 1303–34.

[15] Nogueira H, Adduce C, Alves E, Franca M. Analysis of lock-exchange gravity currents over smooth and rough beds. *J. Hydraulic Res.*, **51**(4), 2013, 417–431.